

Article

Production of Eco-Sustainable Materials: Compatibilizing Action in Poly (Lactic Acid)/High-Density Biopolyethylene Bioblends

Eduardo da Silva Barbosa Ferreira ^{1,*}, Carlos Bruno Barreto Luna ¹, Danilo Diniz Siqueira ¹,
Edson Antonio dos Santos Filho ¹, Edcleide Maria Araújo ¹ and Renate Maria Ramos Wellen ²

¹ Department of Materials Engineering, Federal University of Campina Grande, Campina Grande 58429-900, Brazil; brunobarretodemaufcg@hotmail.com (C.B.B.L.); danilodinizsiqueira@gmail.com (D.D.S.); edson.a.santos.f@gmail.com (E.A.d.S.F.); edcleide.araujo@ufcg.edu.br (E.M.A.)

² Department of Materials Engineering, Federal University of Paraíba, João Pessoa 58051-085, Brazil; wellen.renate@gmail.com

* Correspondence: eduardosbf95@gmail.com

Abstract: Motivated by environment preservation, the increased use of eco-friendly materials such as biodegradable polymers and biopolymers has raised the interest of researchers and the polymer industry. In this approach, this work aimed to produce bioblends using poly (lactic acid) (PLA) and high-density biopolyethylene (BioPE); due to the low compatibility between these polymers, this work evaluated the additional influence of the compatibilizing agents: poly (ethylene octene) and ethylene elastomer grafted with glycidyl methacrylate (POE-g-GMA and EE-g-GMA, respectively), polyethylene grafted with maleic anhydride (PE-g-MA), polyethylene grafted with acrylic acid (PE-g-AA) and the block copolymer styrene (ethylene-butylene)-styrene grafted with maleic anhydride (SEBS-g-MA) to the thermal, mechanical, thermomechanical, wettability and morphological properties of PLA/BioPE. Upon the compatibilizing agents' addition, there was an increase in the degree of crystallinity observed by DSC (2.3–7.6% related to PLA), in the thermal stability as verified by TG (6–15 °C for $T_{D10\%}$, 6–11 °C $T_{D50\%}$ and 112–121 °C for $T_{D99.9\%}$ compared to PLA) and in the mechanical properties such as elongation at break (with more expressive values for the addition of POE-g-GMA and SEBS-g-MA, 9 and 10%, respectively), tensile strength (6–19% increase compared to PLA/BioPE bioblend) and a significant increase in impact strength, with evidence of plastic deformation as observed through SEM, promoted by the PLA/BioPE phases improvement. Based on the gathered data, the added compatibilizers provided higher performing PLA/BioPE. The POE-g-GMA compatibilizer was considered to provide the best properties in relation to the PLA/BioPE bioblend, as well as the PLA matrix, mainly in relation to impact strength, with an increase of approximately 133 and 100% in relation to PLA and PLA/BioPE bioblend, respectively. Therefore, new ecological materials can be manufactured, aiming at benefits for the environment and society, contributing to sustainable development and stimulating the consumption of eco-products.

Keywords: poly (lactic acid); high-density biopolyethylene; bioblends; compatibilization



Citation: Ferreira, E.d.S.B.; Luna, C.B.B.; Siqueira, D.D.; dos Santos Filho, E.A.; Araújo, E.M.; Wellen, R.M.R. Production of Eco-Sustainable Materials: Compatibilizing Action in Poly (Lactic Acid)/High-Density Biopolyethylene Bioblends. *Sustainability* **2021**, *13*, 12157. <https://doi.org/10.3390/su132112157>

Academic Editor: Maria L. Auad

Received: 3 September 2021

Accepted: 12 October 2021

Published: 4 November 2021

Publisher's Note: MDPI stays neutral with regard to jurisdictional claims in published maps and institutional affiliations.



Copyright: © 2021 by the authors. Licensee MDPI, Basel, Switzerland. This article is an open access article distributed under the terms and conditions of the Creative Commons Attribution (CC BY) license (<https://creativecommons.org/licenses/by/4.0/>).

1. Introduction

Motivated by the great research growth of biodegradable and polymers obtained from renewable sources (biopolymers), the study and production of bioblends have gained attention from both industry and polymer scientists, due to its eco-friendly character, as well as the search for new properties, providing new systems with improved performance [1–3]. However, due to the interaction deficiency in the polymer blends, immiscible mixtures are often obtained, exhibiting coarse morphology poorly distributed in the matrix, as also low interfacial adhesion between the phases. Therefore, compatibilization is necessary to modify the interfacial properties of these mixtures, leading to interfacial tension reduction and lower coalescence levels [4–11].

Biodegradable and biopolymers have found a rightful place in the polymer industry due to increased environmental attention, as well as the vast versatility to be used in a range of applications such as biomedical items, packaging and general goods for instance [12,13]. Due to its ability to replace material obtained from non-renewable sources, with high elastic modulus and tensile strength, PLA is the thermoplastic aliphatic polyester among those most studied biodegradable polymers in the last 20 years. Nevertheless, limitations are verified, including low elongation at break and impact strength, low toughness which limit its use in some applications [12,14–17].

Among the biopolymers, biopolyethylene (BioPE), produced by the Brazilian petrochemical Braskem, since 2010, has gained prominence for being considered a technological innovation, due to the reduced dependence on fossil materials, as it comes from sugar cane, as also by the CO₂ absorption from the atmosphere during the production cycle, being chemically and displaying equivalent properties to petroleum-based polyethylene [18–20].

Literature reports works based on the production and characterization of PLA/PE blends [21–27]. Ferri et al. [27] studied PLA/BioPE (80/20) bioblends compatibilized with ethylene vinyl acetate (EVA), polyvinyl alcohol (PVA) and dicumyl peroxide (DCP). Due to immiscibility, the binary blend has reduced mechanical properties compared to PLA, however, upon the addition of three compatibilizers (EVA, PVA and DCP), interactions were improved, and as a consequence, properties increase, such as elongation at break and impact strength. Nevertheless, works based on poly (lactic acid)/high-density polyethylene bioblends from sugarcane together with compatibilizers addition such as POE-g-GMA, EE-g-GMA and SEBS-g-MA are still scarce in the specialized literature, making this research topic pertinent.

With a more demanding society for new green technologies, sustainable consumption is increased by ecological materials. It is a practice related to the acquisition of eco-products that aim to minimize impacts on the environment and, at the same time, maintaining the ecological balance on our planet. In recent years, environmentally responsible practices have become part of the strategy of large companies in the field of polymer technology. In view of the positive contribution to sustainability, bioblends are being developed, aiming at a more sustainable environmental cycle. These are manufactured based on materials from proper environmental sources, with clean production technologies and using renewable sources. Therefore, the environmental, social and economic aspects are justifications for researching the production of these ecological materials.

Based on the above mentioned, the objective of this work was producing PLA/BioPE bioblends compatibilized with several agents, i.e., poly (ethylene octene) grafted with glycidyl methacrylate (POE-g-GMA), ethylene elastomer grafted with glycidyl methacrylate (EE-g-GMA), polyethylene grafted with maleic anhydride (PE-g-MA), polyethylene grafted with acrylic acid (PE-g-AA) and the block copolymer styrene-(ethylene-butylene)-styrene grafted with maleic anhydride (SEBS-g-MA), and evaluating the effect of each compatibilizer in the thermal, mechanical, thermomechanical, wettability and morphology properties of produced bioblends.

2. Methodology

2.1. Materials

Poly (lactic acid) from NatureWorks as pellets with a density of 1.24 g/cm³. High-Density Polyethylene 1'm green SHC7260, from Braskem as pellets with density 0.959 g/cm³, and melting flow rate (MFR) 7.2 g/10 min (190 °C/2.16 kg). As compatibilizing agents: Poly (ethylene octene) grafted with 0.8% glycidyl methacrylate (POE-g-GMA) with trade name Coace W5B from Xiamen Coace Plastic Technology, with density 0.91 g/cm³ and 3 < MFR < 8 g/10 min; Ethylene elastomer grafted with 0.8% glycidyl methacrylate (EE-g-GMA), trade name Coace W5D, with density 0.92 g/cm³ and 8 < MFR < 16 g/10 min from Xiamen Coace Plastic Technology; Polyethylene grafted with 1.5–1.7% Maleic Anhydride (PE-g-MA) marketed as Polybond 3029, MFR 4 g/10 min supplied by Addivant; Polyethylene grafted with 5.5–6.5% Acrylic Acid (PE-g-AA) marketed as Polybond 1009,

MFR 5 g/10 min supplied by Addivant, and styrene(ethylene-butylene)-styrene functionalized block copolymer with 1.7% maleic anhydride (SEBS-g-MA) marketed as Kraton[®] FG1901G with MFR 5 g/10 min (200 °C/5 kg), supplied by the Kraton Polymers Group of Companies.

2.2. Bioblends Processing

Processed bioblends with compositions and codes are shown in Table 1. Initially, bioblends components were manually cold-mixed in order to promote greater homogenization, then extruded using a co-rotational, interpenetrating, modular ZSK model twin-screw extruder (D = 18 mm and L/D = 40), Werner-Pfleiderer, Coperion (Stuttgart, Germany). The processing parameters are shown in Table 2. The screw profile used was configured with distributive and dispersive modules, for better mixture homogeneity.

Table 1. Compositions of binary and compatible bioblends with mass proportion (%).

Samples	PLA (%)	BioPE (%)	POE-g-GMA (%)	EE-g-GMA (%)	PE-g-MA (%)	PE-g-AA (%)	SEBS-g-MA (%)
PLA	100	-	-	-	-	-	-
BioPE	-	100	-	-	-	-	-
PLA/BioPE	70	30	-	-	-	-	-
PLA/BioPE/POE-g-GMA	70	20	10	-	-	-	-
PLA/BioPE/EE-g-GMA	70	20	-	10	-	-	-
PLA/BioPE/PE-g-MA	70	20	-	-	10	-	-
PLA/BioPE/PE-g-AA	70	20	-	-	-	10	-
PLA/BioPE/SEBS-g-MA	70	20	-	-	-	-	10

Table 2. Applied parameters during extrusion and injection processing.

Parameters			
Extrusion		Injection	
Feed rate (kg/h)	3	Injection and hold pressing (bar)	800 and 500
Temperature profile (°C)	170, 170, 175, 175, 175, 180, 180	Temperature profile (°C)	170, 175, 175, 180, 180
Screw rate (rpm)	250	Mold temperature (°C)	20

The extruded was pelletized and vacuum dried at 60 °C for 24 h. Afterwards, specimens were injection molded using an Arburg Model Allrounder 207C Golden Edition injection molding machine (Radevormwald, Germany). Tensile, impact, and heat deflection temperature (HDT) specimens were molded according to ASTM D638 (Type I), ASTM D256, and ASTM D648, respectively. Table 2 presents applied parameters during extrusion and specimen injection.

2.3. Characterizations

Differential scanning calorimetry (DSC) analyses were carried out using a TA Instruments DSC-Q20 (New Castle, United States), and samples were heated from room temperature (~23 °C) to 200 °C, at 10 °C/min, under a nitrogen atmosphere with gas flow 50 mL/min. Tested samples were approximately 5 mg weight. The degree of crystallinity (X_c) of produced samples was calculated according to Equation (1) [28]:

$$X_c(\%) = \frac{\Delta H_m - \Delta H_{cc}}{W \times \Delta H_m^0} \times 100 \quad (1)$$

where: ΔH_m is the melting enthalpy of PLA and BioPE; ΔH_{cc} is the cold crystallization enthalpy; ΔH^0 is equilibrium melting enthalpy, where 100% crystalline PLA is 93.7 J/g [29], and 100% crystalline BioPE is 290 J/g [30]; W is the matrix content.

Plots of molten fraction and melting rate were acquired through DSC peaks integration using INTEGRAL software, and Equations (2)–(4). The molten fraction (x) as time function (t) is given by the area between (J) and a virtual baseline during the event (J_0), defined as the straight line between the start and end points, where E_0 is the total latent heat of the phase change; and t_1 and t_2 are the start and end times of the event, respectively [31–33]:

$$x(t) = \frac{1}{E_0} \int_{t_1}^t |J(t') - J_0(t')| dt' \quad (2)$$

where:

$$E_0 = \int_{t_1}^{t_2} |J(t) - J_0(t)| dt \quad (3)$$

Molten fraction can be expressed as temperature function (T), knowing the linear relationship between time and temperature during the event: $T = T_1 + \varphi (t - t_1)$, where T_1 is the sample temperature at the initial point t_1 , $\tau = t - t_1$ is the time measured since the event start, and $\varphi = dT/dt$ is the heating/cooling rate (constant) during the event. Therefore, the melting rate (C_m) can be given by Equation (4), from which the melting rate was computed [31–33]:

$$c_m = \frac{dx}{dt} = \frac{|J(t) - J_0(t)|}{E_0 \varphi} \quad (4)$$

Thermogravimetry (TG) analyses carried out in a TA Instruments SDT Q600 simultaneous TG/DSC device (Kyoto, Japan) employing samples with 5 mg, heated from room temperature ($\sim 23^\circ\text{C}$) to 500°C , the heating rate was $10^\circ\text{C}/\text{min}$ and nitrogen flow rate of $100\text{ mL}/\text{min}$.

Tensile test was performed on injected specimens according to ASTM D638 using an EMIC DL 2000 (São José dos Pinhais, Brazil) universal testing machine with an elongation rate of $50\text{ mm}/\text{min}$ and load cell of 20 kN at room temperature ($\sim 23^\circ\text{C}$). Presented results are an average of ten specimens.

Izod impact strength measurements were performed based on ASTM D256-97 using notched specimens in a Ceast Resil 5.5 J device (Turin, Italy) operating with 2.75 J hammer at room temperature ($\sim 23^\circ\text{C}$). Presented results are an average of ten specimens.

Heat deflection temperature (HDT) was evaluated according to ASTM D648, in a Ceast model HDT 6 VICAT (Turin, Italy) with a voltage of 1.82 MPa , and heating rate $120^\circ\text{C}/\text{h}$ (method A). HDT was determined after specimen deflecting 0.25 mm . Presented results are an average of three specimens.

Vicat softening temperature (VST) test carried out according to the ASTM D1525 standard, in Ceast equipment (Turin, Italy), model HDT 6 VICAT/N 6921.000, at a heating rate of $120^\circ\text{C}/\text{h}$. VST was determined after the needle penetrating 1 mm into the specimens. Reported results are an average of three experiments.

Shore D hardness test carried out according to the ASTM D2240 standard, on Shore-Durometer Hardness Type "D" Woltest (São Paulo, Brazil), with 50 N load controlled by calibrated springs using standardized indenters. Reported results are an average of five experiments.

The contact angle analysis was performed using the sessile drop method, using a portable contact angle; model Phoenix-i from Surface Electro Optics–SEO (Gyeonggi-do, South Korea). The drop was deposited on impact specimens using a micrometric meter; the image was captured and analyzed through the equipment software.

Scanning electron microscopy (SEM) images were captured on the fractured surface from the impact test. A scanning electron microscope, VEGA 3 TESCAN (Brno, Czech Republic), at a voltage of 30 kV under a high vacuum was used. Fractured surfaces were gold coated.

3. Results and Discussion

3.1. Differential Scanning Calorimetry (DSC)

DSC scans acquired during cooling and second heating for PLA, BioPE, PLA/BioPE and compatibilized bioblends are displayed in Figure 1 and the computed parameters are informed in Table 3.

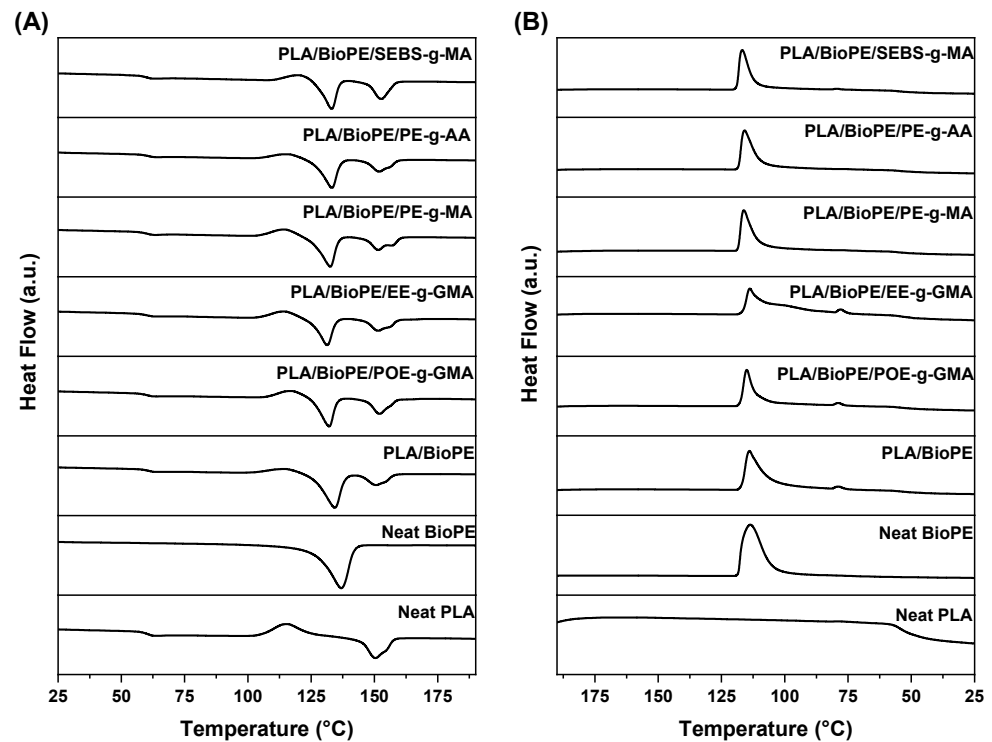


Figure 1. DSC scans acquired during the second heating (A) and cooling (B) of PLA, BioPE, PLA/BioPE and compatibilized bioblends.

Table 3. Melting and crystallization parameters of investigated samples.

Samples	T_g (°C)	T_m^1 (°C)	T_m^2 (°C)	ΔH_m^1 (J/g)	ΔH_m^2 (J/g)	X_c (%)	T_{cc} (°C)	ΔH_{cc} (J/g)	T_c (°C)
PLA	61	150.4	-	24.5	-	3.9	115.4	20.8	-
BioPE	-	-	136.8	-	176.1	60.1	-	-	113.6
PLA/BioPE	61	150.7	134.3	13.4	39.7	9.4	114.8	7.2	113.9
PLA/BioPE/POE-g-GMA	60	152.7	132.1	16.5	26.1	9.3	117.3	10.4	115
PLA/BioPE/EE-g-GMA	59	151.4	131.3	16.1	27.1	6.2	114.7	12	113.8
PLA/BioPE/PE-g-MA	60	151.6	132.5	19	32.8	11.4	114.7	11.5	116.1
PLA/BioPE/PE-g-AA	61	151.9	133.2	15.4	32.7	10.9	115.8	8.3	115.9
PLA/BioPE/SEBS-g-MA	60	152.7	133.1	16.5	23.1	11.5	120.4	8.9	116.8

T_g is the glass transition temperature; T_m^1 PLA melting peak temperature; T_m^2 BioPE melting peak temperature; ΔH_m^1 PLA melting enthalpy; ΔH_m^2 BioPE melting enthalpy; X_c degree of crystallinity; T_{cc} cold crystallization temperature; ΔH_{cc} cold crystallization enthalpy; T_c melting crystallization temperature.

For PLA during heating, from the glass transition temperature (T_g) around 57–62 °C, an exothermic peak immediately before melting originating from the cold crystallization of the disordered α phase, then an endothermic peak ranging from 115.4 to 150.4 °C is observed in Figure 1A [34]. DSC scans of BioPE samples show the endothermic peak due to the melting with peak temperature at 136.8 °C, and the exothermic peak during cooling due to the melting crystallization with the temperature at 113.6 °C [35]. For PLA/BioPE samples, DSC scans displayed the exothermic and endothermic peaks characteristic of the individual polymers, whether compatibilized or not. The degree of crystallinity was

evaluated through Equation (1); the results are presented in Table 3 together with associated parameters of the phase transitions.

PLA presented a low degree of crystallinity, i.e., X_c 3.9% whereas for BioPE high values were computed, i.e., X_c 60.1%. For bioblends, X_c increased, suggesting that the presence of BioPE increases the mobility of PLA chains, as well as the addition of compatibilizers, in response to the interactions developed between the macromolecular chains of PLA, BioPE and the compatibilizers, which tend to increase miscibility of samples [27].

Figure 2 illustrates the molten fraction and melting rate of the PLA-rich phase as temperature function. Parameters $T_{0.01}$, $T_{0.99}$ and C_{max} are shown in Table 4.

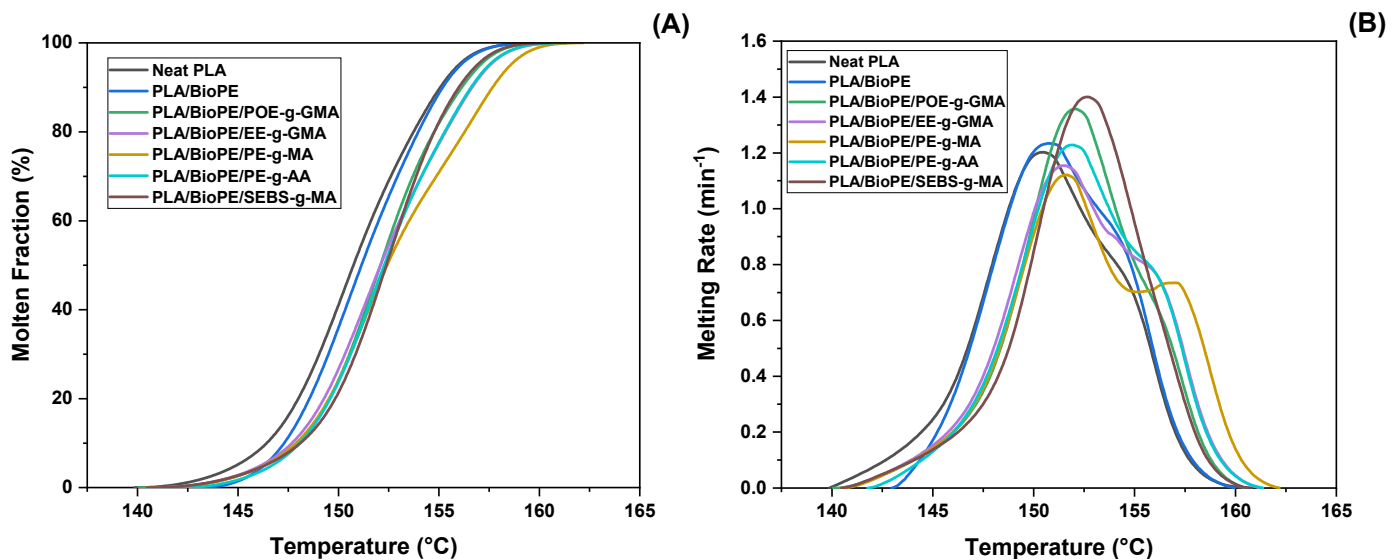


Figure 2. Molten fraction (A) and Melting rate (B) of investigated samples.

Table 4. Computed parameters from Figure 2 for the investigated samples.

Samples	$T_{0.01}$ (°C)	$T_{0.99}$ (°C)	C_{max} (min^{-1})
PLA	139.8	160.2	1.19
PLA/BioPE	142.9	159.9	1.22
PLA/BioPE/POE-g-GMA	140.4	160.4	1.35
PLA/BioPE/EE-g-GMA	140.6	161.1	1.15
PLA/BioPE/PE-g-MA	140.5	162.1	1.11
PLA/BioPE/PE-g-AA	141.8	161.3	1.21
PLA/BioPE/SEBS-g-MA	140.5	160.5	1.40

$T_{0.01}$ initial melting temperature; $T_{0.99}$ final melting temperature; C_{max} maximum melting rate.

Molten fraction displayed a sigmoidal character suggesting that the phase transition took place without discontinuities. In general, bioblends displayed subtle higher $T_{0.01}$ related to PLA. For $T_{0.99}$, there is a maintenance in relation to the neat PLA, with small increases for the compatibilized bioblends in relation to the binary bioblend. Regarding the melting rate Figure 2B, the bioblends compatibilized with POE-g-GMA and SEBS-g-MA showed the highest maximum melting rate (C_{max}) results both in relation to neat PLA and also to PLA/BioPE.

3.2. Thermogravimetry (TG)

Figure 3 presents TG plots of investigated samples and computed parameters from these plots are displayed in Table 5.

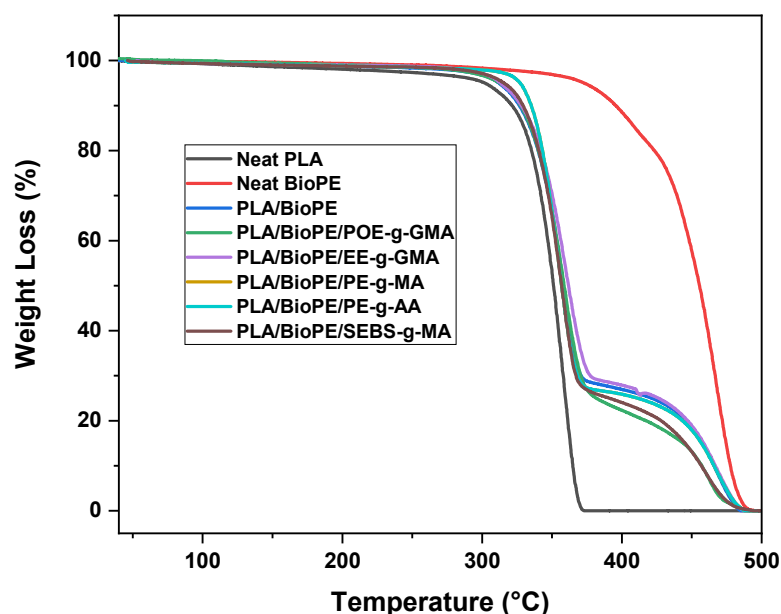


Figure 3. TG plots of investigated samples.

Table 5. $T_{D10\%}$, $T_{D50\%}$ and $T_{D99.9\%}$ parameters under inert atmosphere (N_2) and heating rate $10\text{ }^\circ\text{C}/\text{min}$.

Samples	$T_{D10\%}$ ($^\circ\text{C}$)	$T_{D50\%}$ ($^\circ\text{C}$)	$T_{D99.9\%}$ ($^\circ\text{C}$)
PLA	320	350	373
BioPE	395	455	496
PLA/BioPE	326	358	485
PLA/BioPE/POE-g-GMA	327	358	490
PLA/BioPE/EE-g-GMA	328	361	487
PLA/BioPE/PE-g-MA	335	356	488
PLA/BioPE/PE-g-AA	335	356	487
PLA/BioPE/SEBS-g-MA	329	356	494

$T_{D10\%}$ = temperature for 10% of decomposed material. $T_{D50\%}$ = temperature for 50% of decomposed material. $T_{D99.9\%}$ = temperature for 99.9% of decomposed material.

From Figure 3 it is observed that neat polymers presented a single decomposition step, around $300\text{--}373\text{ }^\circ\text{C}$ for PLA [36–38], and $350\text{--}496\text{ }^\circ\text{C}$ for BioPE [35]. For PLA/BioPE bioblend, two decomposition steps were verified, where each decomposition step is characteristic of the individual polymer, i.e., PLA and BioPE. The compatibilized bioblends presented similar behavior to PLA/BioPE, however, as shown in Table 5, there was a subtle increase in $T_{D10\%}$ and $T_{D99.9\%}$, and small decrease in $T_{D50\%}$ for the compatibilized samples with PE-g-MA, PE-g-AA and SEBS-g-MA. It is worth noting that all bioblends had $T_{D10\%}$, $T_{D50\%}$ and $T_{D99.9\%}$ greater than neat PLA, with PLA/BioPE/PE-g-MA and PLA/BioPE/PE-g-AA bioblends having the highest values of $T_{D10\%}$ ($335\text{ }^\circ\text{C}$), the bioblend PLA/BioPE/EE-g-GMA with the highest $T_{D50\%}$ ($361\text{ }^\circ\text{C}$) and PLA/BioPE/SEBS-g-MA with the highest $T_{D99.9\%}$ ($494\text{ }^\circ\text{C}$).

Therefore, gathered results indicate that the compatibilizing agents' addition to PLA/BioPE bioblend tends to improve the thermal stability not only in relation to PLA, but also to the binary bioblend, with improvement and/or maintenance of $T_{D10\%}$, $T_{D50\%}$ and $T_{D99.9\%}$ as reported.

3.3. Tensile Test

Elastic modulus data acquired under tension are illustrated in Figure 4. PLA and BioPE had an elastic modulus of 1221 and 376 MPa, respectively, with PLA having the highest stiffness [37,38], and BioPE increased flexibility, results corroborating these are

shown later on for impact strength. PLA/BioPE due to the addition of 30% of a ductile material to PLA matrix, displayed decaying of 26.8% on the material's stiffness compared to PLA, i.e., it presented 893 MPa. In general, upon compatibilizing agent addition, the results were quite similar to PLA/BioPE, similar to those observed by Ferri et al. [27].

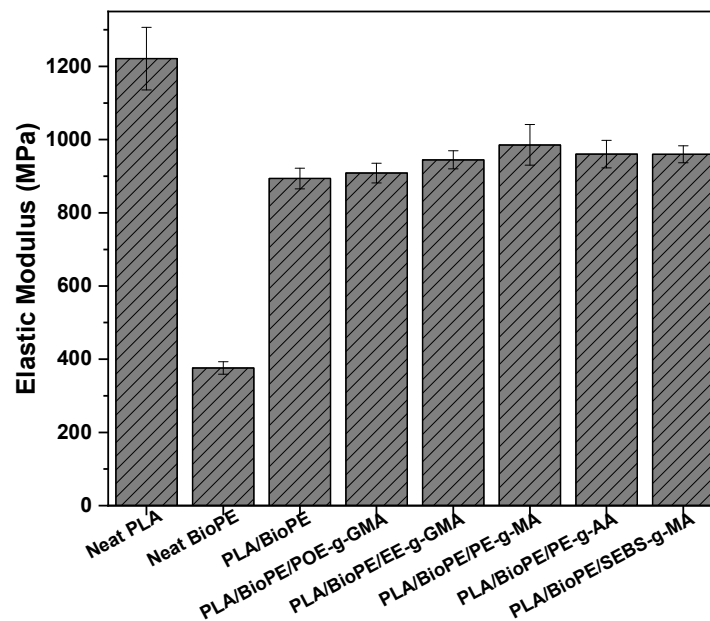


Figure 4. Elastic Modulus of investigated samples.

Figure 5 shows collected results for tensile strength. It is verified that PLA and BioPE have the highest and lowest tensile strength, respectively, i.e., 60 and 21 MPa, which are expected due to the fact that PLA has brittle material character requiring high stress to fracturing, while BioPE has ductile character. For PLA/BioPE bioblend (32 MPa), there was a considerable decrease compared to PLA, due to the addition of less rigid material, as well as due to poor adhesion between the phases of the system [39]. It may be observed that upon addition of the compatibilizers POE-g-GMA, EE-g-GMA, PE-g-MA, PE-g-AA and SEBS-g-MA, there was an increase in tensile strength, when compared to PLA/BioPE bioblends, for 38, 35, 39, 35 and 38 MPa, respectively, being directly linked to better adhesion between the phases present in the system, corroborating the impact strength results and the SEM images, which will be noted in later sections.

Figure 6 shows acquired results for the elongation at break of investigated samples. Differences are observed in relation to PLA/BioPE without and with compatibilizing agents. PLA/BioPE presented an elongation at break of 6.9%, bioblends compatibilized with POE-g-GMA, EE-g-GMA, PE-g-MA, PE-g-AA and SEBS-g-MA presented values of 9%, 8.7%, 8.3%, 8% and 10%, respectively. The increase in this property is related to the improvement in the stress transfer between the matrix and the dispersed phase of studied systems, due to the improvement in the interactions among the chemical groups present in the compatibilizers, showing its effectiveness [40,41]. These results corroborate those presented later on for impact strength, where the addition of POE-g-GMA, EE-g-GMA and SEBS-g-MA presented the best impact strengths, as well as higher elongations at break.

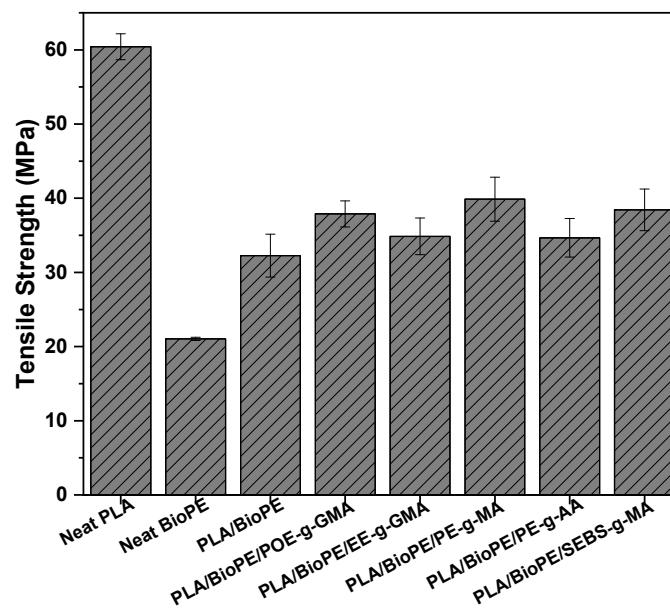


Figure 5. Tensile strength of investigated samples.

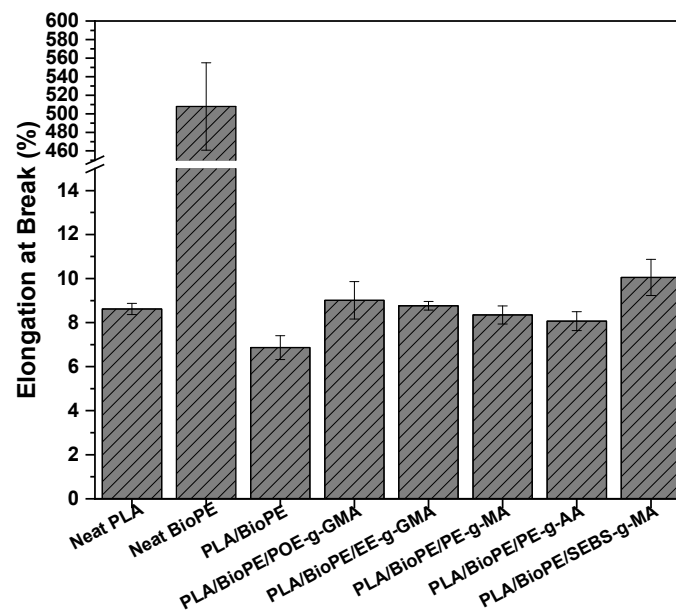


Figure 6. Elongation at break of investigated samples.

3.4. Impact Strength

Figure 7 illustrates the impact strength results obtained for the investigated samples. PLA displayed a typical fragile character with low energy dissipation with an impact strength of 27 J/m, which is in agreement with those already reported [12,14–16,27,38,42,43], and corroborated through SEM images later on presented (Figure 11). BioPE presented a typical ductile character with an impact strength of approximately 98 J/m [35]. Upon addition of 30% BioPE to PLA, there was an increase of 20% for PLA/BioPE related to PLA, even with the poor adhesion between the phases (see Figure 11).

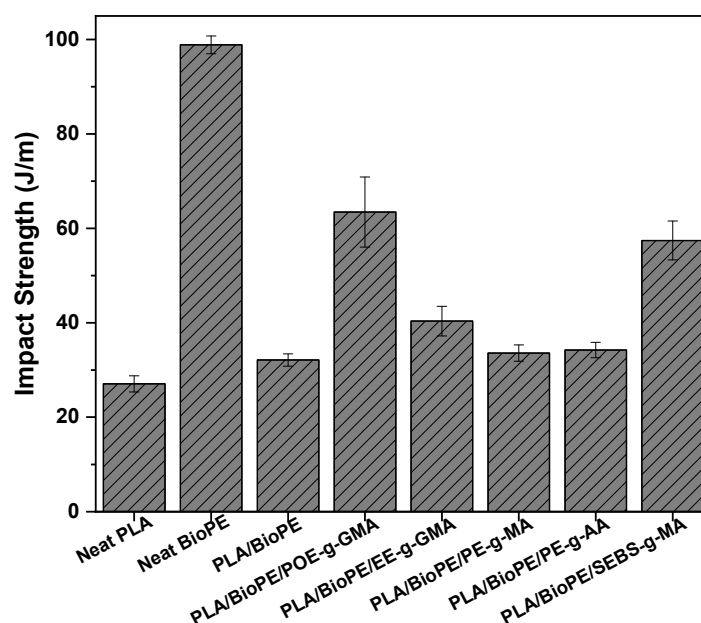


Figure 7. Impact strength of investigated samples.

For the compatibilized bioblends, impact strength increased with the addition of POE-g-GMA, EE-g-GMA and SEBS-g-MA, and remained unchanged with the addition of PE-g-MA and PE-g-AA. For compatibilizers grafted with GMA there was an increase of 100% for POE-g-GMA (~64 J/m) and approximately 30% for EE-g-GMA (~41 J/m), when compared to PLA/BioPE. This considerable improvement in toughness with the compatibilizers addition containing GMA is suggested to be related to chemical reactions between GMA epoxy groups and the terminal hydroxyl or carboxyl groups of PLA [24]. Upon SEBS-g-MA addition there was an increase of 78% compared to the bioblend without compatibilizer, with an impact strength of approximately 58 J/m, due to the fact that SEBS has elastomeric characteristic, and it is able to develop interactions between the phases with the elastomer grafted with MA, increasing the compound ductility.

Increases in impact strength were also observed in the reports of Ferri et al. [27] and Quiles et al. [44] in blends with PLA and PE, when added compatibilizers. Demonstrating the importance of adding a third phase to the immiscible PLA/BioPE system to improve properties such as toughness for example. Comparing the compatibilizers in relation to the degree of grafting of GMA, MA and AA, it may be verified that even using low levels of grafting of GMA (0.8%) for the compatibilizers POE-g-GMA and EE-g-GMA, compared to the highest MA contents (1.5–1.7 and 1.7%) for PE-g-MA and SEBS-g-MA, respectively, and AA (5.5–6.5%) for PE-g-AA, the predominant factor was the elastomeric characteristic of the used copolymers, with greater gains upon addition of POE-g-GMA and SEBS-g-MA.

The impact strength results of PLA/BioPE/POE-g-GMA and PLA/BioPE/SEBS-g-MA bioblends are relevant from a technological point of view, as they surpass the impact strength values of widely used commodity polymers in the development of products such as polypropylene (PP) [45–47], polystyrene (PS) [48,49] and polyamide 6 (PA6) [50–52]. From a sustainable point of view, it is extremely important, as polymers from renewable sources such as PLA and BioPE are being used in the bioblend, being an alternative for the use of the aforementioned polymers.

3.5. Heat Deflection Temperature (HDT)

The heat deflection temperature (HDT) becomes an important parameter for higher temperatures applications being an indication of the dimensional stability of the material under the effect of a specific load and temperature increasing [38,53].

Figure 8 presents HDT for the investigated samples. For PLA, HDT was 56 °C, a consequence of its glass transition temperature (T_g), as observed in the DSC scans [54,55].

BioPE had lower HDT (52 °C), being influenced, in this case, directly by the stiffness of the system, as observed in Figure 4, presenting the lowest value of elastic modulus among the studied samples. Upon addition of 30% BioPE to PLA matrix, HDT decayed only 1 °C compared to PLA. Upon addition of 10% of compatibilizer to PLA/BioPE, regardless of the compatibilizer, HDT decayed only 1 °C, related to PLA/BioPE. Therefore, comparing bioblends with PLA, there were no significant decreases in HDT, which is important from a technological and scientific point of view, an important parameter in the polymer industry, as well as linked to the significant increase in the material toughness as observed by the impact strength, especially for POE-g-GMA and SEBS-g-MA compatibilizers.

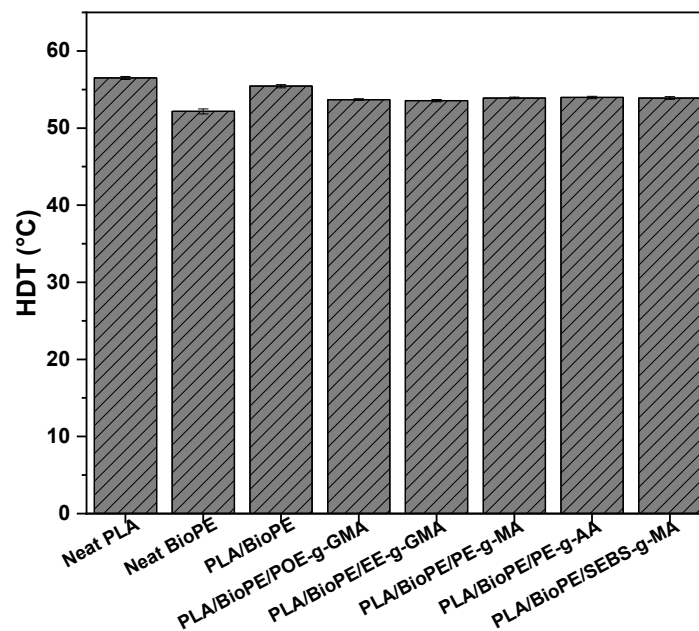


Figure 8. HDT of investigated samples.

3.6. Vicat Softening Temperature (VST) and Shore D Hardness

Similar to HDT, the Vicat softening temperature is considered an important property in polymeric systems, during production and projection of industrial applications aimed at thermomechanical resistance, being the temperature at which a needle penetrates the sample 1 mm, under a specific load, being mostly of materials, directly proportional to their surface hardness [53,56]. Figure 9 shows the relationship between VST and Shore D hardness of the investigated samples.

PLA presented VST around 59 °C, close to HDT. Upon temperature increase, the material goes from the solid to the rubbery state, hence reaching T_g , the needle penetrates the specimen. Shore D hardness testing is performed at room temperature; solid PLA has high surface hardness (69). Regarding BioPE, it displayed low hardness as it is a material with low stiffness, as observed in the tensile results, and high VST due to high crystallinity as verified through DSC [57].

For PLA/BioPE bioblend, Shore D hardness decreased whereas VST was unchanged, corroborating the decrease in stiffness provided by the BioPE phase, as also observed by Ferri et al. [27]. For the compatibilized bioblends, Shore D hardness results were similar to each other, being within the experimental error, while VST results decreased in relation to PLA/BioPE, with a reduction from 59 °C to 55–57 °C, probably due to T_g reduction, as seen in Table 3.

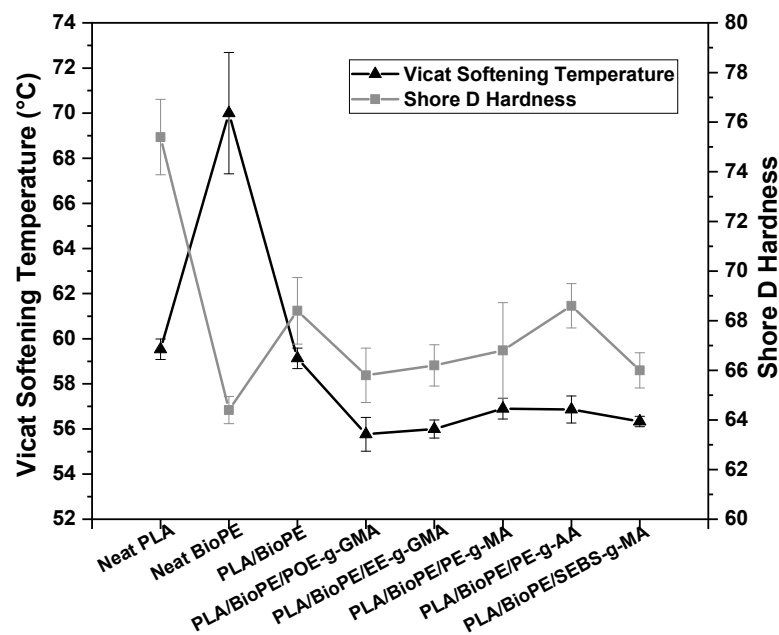


Figure 9. VST and Shore D Hardness of investigated samples.

3.7. Contact Angle

The contact angle results for the investigated materials are shown in Figure 10. The contact angle, in addition to enabling the assessment of the hydrophilicity or hydrophobicity of a material [38,58,59], also allows the assessment of surface energy [60], which is an important parameter during the production of compatible bioblends.

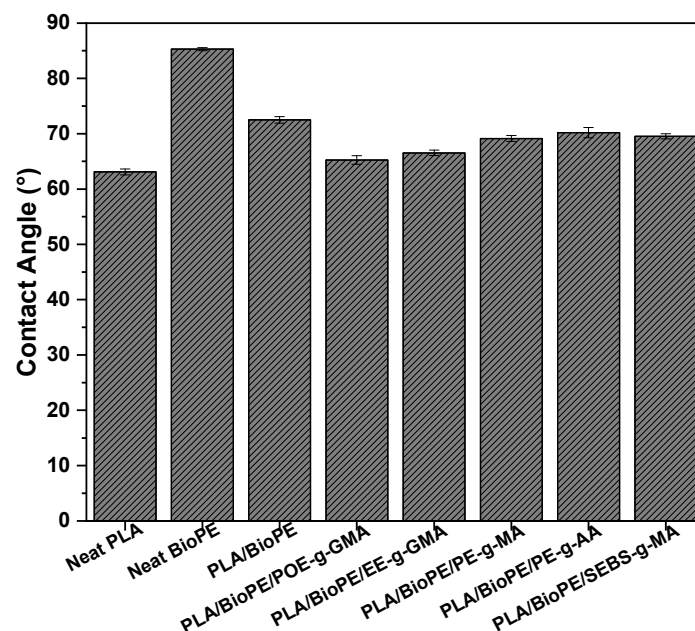


Figure 10. Contact angle of investigated samples.

Figure 10 shows the acquired data for the contact angle, where PLA displayed a value of 63° , and BioPE 85° , confirming greater hydrophobicity for BioPE, and PLA has chemical groups (hydroxyl and carboxyl), interacting with water, hence leading to smaller contact angle. PLA/BioPE bioblends presented an intermediate contact angle related to neat polymers, being approximately 72° . Upon compatibilizers addition, the contact angle decreased, in relation to PLA/BioPE bioblend, due to the increase in the interfacial and surface interactions, corroborating the results of impact strength and SEM. It is worth

mentioning that chemical groups such as GMA, MA and AA present in the used compatibilizing agents, in addition to interacting with PLA and BioPE, tend to interact with water, increasing surface wettability and thus decreasing the contact angle of the systems in relation to PLA/BioPE bioblend.

3.8. Scanning Electron Microscopy (SEM)

SEM images of the specimens fractured surface from impact strength testing, of PLA, BioPE, PLA/BioPE and compatibilized bioblends are shown in Figure 11, with 500 and 1000 \times magnification for PLA, and 2000 and 5000 \times for the other samples.

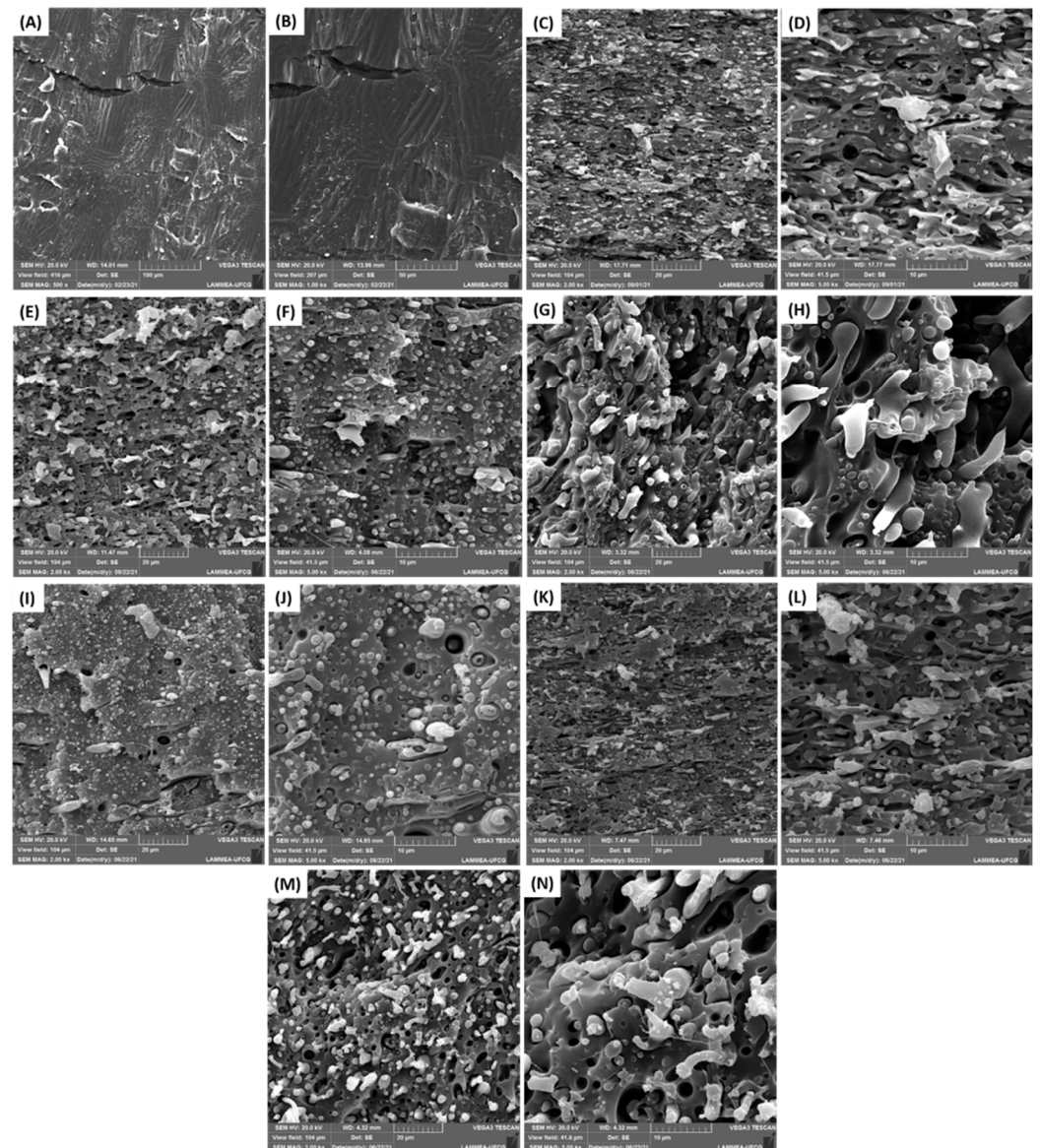


Figure 11. SEM images of PLA (A,B), PLA/BioPE (C,D), bioblends compatibilized with POE-g-GMA (E,F), EE-g-GMA (G,H), PE-g-MA (I,J), PE-g-AA (K,L) and SEBS-g-MA (M,N). Images are 500 and 1000 \times magnification of neat PLA, and 2000 and 5000 \times for the other compositions.

Regarding PLA (Figure 11a,b), smooth surface without roughness was observed, due to the absence of plastic deformation, characteristic of fragile fracture, as observed in the impact strength and tensile experiments [37,38,61–63].

SEM images of PLA/BioPE without compatibilizer showed immiscibility and poor adhesion between PLA and BioPE polymers, with BioPE particles pulled out from PLA

matrix, with presence of voids in the fracture surface, promoting low tensile and impact strength properties [24,27].

For the compatibilized bioblends, the roughness was verified on the specimens' surfaces, characteristic of plastic deformation, mainly for PLA/BioPE/POE-g-GMA, PLA/BioPE/EE-g-GMA and PLA/BioPE/SEBS-g-MA, due to the elastomeric character present in the copolymer, resulting in more elongated particles after the impact test. Related to the addition of PE-g-MA and PE-g-AA compatibilizers, there was lower surface roughness, with homogeneity when compared to the PLA/BioPE bioblend, due to the presence of MA and AA groups, resulting in improvement in interactions as well as good tensile strength results, mainly for PE-g-AA, but with the maintenance of impact strength compared to PLA/BioPE bioblend. Thus, it was observed that the elastomeric character of the copolymers was predominant in the best impact strength results compared to PLA/BioPE bioblend, that is, the compatibilizers POE-g-GMA, EE-g-GMA, and SEBS-g-GMA obtained the best impact strength results, not only due to the improved interactions between PLA and GMA and MA groups, but also due to the elastomeric character of these copolymers.

4. Conclusions

The addition effect of POE-g-GMA, EE-g-GMA, PE-g-MA, PE-g-AA and SEBS-g-MA on the thermal, mechanical, thermomechanical properties, wettability (contact angle) and morphology of PLA/BioPE bioblends was investigated. Regarding thermal analysis, it was observed by DSC that the BioPE addition as well as compatibilizing agents increase the degree of crystallinity of neat PLA, increase the macromolecular chains, and provide significant improvement in thermal stability, mainly in parameter $T_{D99.9\%}$, as observed by TG. The mechanical and thermomechanical properties demonstrated that the compatibilizing agents improve the interactions among bioblends phases, with property increases such as elongation at break, tensile strength, impact strength, and unchanged elastic modulus, related to PLA/BioPE. Through contact angle measurements, an increase in wettability was observed compared to PLA/BioPE. SEM images showed that the addition of POE-g-GMA, EE-g-GMA and SEBS-g-MA considerably increased the roughness, promoting plastic deformation and better impact strength performance related to PLA/BioPE and PLA. The addition of POE-g-GMA compatibilizer to PLA/BioPE displayed the best overall balance in relation to the investigated properties. Acquired results indicate that PLA/BioPE needs to be compatibilized in order to promote interactions among phases, and consequently improve the technological performance. The manufacture of bioblends is an alternative for the commercialization of eco-products that contribute to a friendlier environmental cycle.

Author Contributions: All authors participated in the drafting the article or revising it critically content, approving the final version submitted. Conceptualization, E.d.S.B.F., C.B.B.L., E.M.A. and R.M.R.W.; methodology, E.d.S.B.F., D.D.S., and E.A.d.S.F.; formal analysis, E.d.S.B.F., C.B.B.L. and E.A.d.S.F.; investigation, E.d.S.B.F., C.B.B.L. and D.D.S.; resources, E.M.A.; writing—original draft preparation, E.d.S.B.F. and C.B.B.L.; writing—review and editing, E.d.S.B.F. and E.M.A. and R.M.R.W.; visualization, E.d.S.B.F. and C.B.B.L.; supervision, E.M.A.; project administration, E.M.A. and R.M.R.W.; funding acquisition, E.M.A. All authors have read and agreed to the published version of the manuscript.

Funding: The authors are grateful to CNPq (National Council for Scientific and Technological Development, Brasilia/DF, Brazil) and CAPES (Coordination for the Improvement of Higher Education Personnel, Brasilia/DF, Brazil) for the financial support. Edcleide Araújo and Renate Wellen are CNPq fellows.

Acknowledgments: The author would to thank Addivant for PE-g-MA and PE-g-AA donation; Xiamen Coace Plastic Technology for POE-g-GMA and EE-g-GMA donation and Kraton Polymers Group of Companies for SEBS-g-MA donation and FAPESQ for support. The authors thank UFCG for paying the publication fee.

Conflicts of Interest: There is no conflict of interest and all authors have agreed with this submission and they are aware of the content.

References

1. Mohamed, A.; Gordon, S.H.; Biresaw, G. Polycaprolactone/polystyrene bioblends characterized by thermogravimetry, modulated differential scanning calorimetry and infrared photoacoustic spectroscopy. *Polym. Degrad. Stab.* **2007**, *92*, 1177–1185. [[CrossRef](#)]
2. Al-Itry, R.; Lamnawar, K.; Maazouz, A. Biopolymer Blends Based on Poly (lactic acid): Shear and Elongation Rheology/Structure/Blowing Process Relationships. *Polymers* **2015**, *7*, 939–962. [[CrossRef](#)]
3. Olejnik, O.; Masek, A.; Zawadzko, J. Processability and Mechanical Properties of Thermoplastic Polylactide/Polyhydroxybutyrate (PLA/PHB) Bioblends. *Materials* **2021**, *14*, 898. [[CrossRef](#)]
4. Kim, Y.F.; Choi, C.N.; Lee, K.Y.; Lee, M.S. Compatibilization of immiscible poly(l-lactide) and low density polyethylene blends. *Fibers Polym.* **2004**, *5*, 270–274. [[CrossRef](#)]
5. La Mantia, F.P.; Morreale, M.; Botta, L.; Mistretta, M.; Ceraulo, M.; Scaffaro, R. Degradation of polymer blends: A brief review. *Polym. Degrad. Stab.* **2017**, *145*, 79–92. [[CrossRef](#)]
6. Effah, B.; Van Reenen, A.; Meincken, M. Mechanical properties of wood-plastic composites made from various wood species with different compatibilizers. *Eur. J. Wood Wood Prod.* **2018**, *76*, 57–68. [[CrossRef](#)]
7. Luna, C.B.B.; Siqueira, D.D.; Araújo, E.M.; Wellen, R.M.R. Tailoring PS/PPrecycled blends compatibilized with SEBS. Evaluation of rheological, mechanical, thermomechanical and morphological characters. *Mater. Res. Express* **2019**, *6*, 075316. [[CrossRef](#)]
8. Czarnecka-Komorowska, D.; Nowak-Grzebyta, J.; Gawdzińska, K.; Mysiukiewicz, O.; Tomasik, M. Polyethylene/Polyamide Blends Made of Waste with Compatibilizer: Processing, Morphology, Rheological and Thermo-Mechanical Behavior. *Polymers* **2021**, *13*, 2385. [[CrossRef](#)]
9. Ferreira, E.D.S.B.; Luna, C.B.B.; Araújo, E.M.; Siqueira, D.D.; Wellen, R.M.R. Polypropylene/wood powder/ethylene propylene diene monomer rubber-maleic anhydride composites: Effect of PP melt flow index on the thermal, mechanical, thermomechanical, water absorption, and morphological parameters. *Polym. Compos.* **2021**, *42*, 484–497. [[CrossRef](#)]
10. Silva, P.T.V.; Luna, C.B.B.; Ferreira, E.S.B.; Santos Filho, E.A.; Araújo, E.M. Evolution of morphology and mechanical properties of PA6/AES blends compatibilized with EPDM-MA. *Res. Soc. Dev.* **2021**, *10*, e210101018791. [[CrossRef](#)]
11. Nogueira, J.A.S.; Luna, C.B.B.; Siqueira, D.D.; Santos Filho, E.A.; Araújo, E.M. Performance investigation of PA6/HIPS blends compatibilized with SEBS-MA. Effect of compatibilizer content on mechanical, thermomechanical, torque rheometry and morphology properties. *Res. Soc. Dev.* **2021**, *10*, e58510817649.
12. Saini, P.; Arora, M.; Kumar, M.R. Poly(lactic acid) blends in biomedical applications. *Adv. Drug Deliv. Rev.* **2016**, *107*, 47–59. [[CrossRef](#)] [[PubMed](#)]
13. Ye, G.; Wang, W.; Fan, D.; He, P. Effects of femtosecond laser micromachining on the surface and substrate properties of poly-lactic acid (PLA). *Appl. Surf. Sci.* **2021**, *538*, 148117. [[CrossRef](#)]
14. Garlotta, D. A Literature Review of Poly(Lactic Acid). *J. Polym. Environ.* **2001**, *9*, 63–84. [[CrossRef](#)]
15. Gigante, V.; Canesi, I.; Cinelli, P.; Coltelli, M.B.; Lazzeri, A. Rubber Toughening of Poly(lactic acid) (PLA) with Poly(butylene adipate-co-terephthalate) (PBAT): Mechanical Properties, Fracture Mechanics and Analysis of Ductile-to-Brittle Behavior while Varying Temperature and Test Speed. *Eur. Polym. J.* **2019**, *115*, 125–137. [[CrossRef](#)]
16. Wu, F.; Misra, M.; Mohanty, A.K. Super Toughened Poly(lactic acid)-Based Ternary Blends via Enhancing Interfacial Compatibility. *ACS Omega* **2019**, *4*, 1955–1968. [[CrossRef](#)]
17. McKeown, P.; Jones, M.D. The Chemical Recycling of PLA: A Review. *Sustain. Chem.* **2020**, *1*, 1. [[CrossRef](#)]
18. Boronat, T.; Fombuena, V.; Garcia-Sanoguera, D.; Sanchez-Nacher, L.; Balart, R. Development of a biocomposite based on green polyethylene biopolymer and eggshell. *Mater. Des.* **2015**, *68*, 177–185. [[CrossRef](#)]
19. Spalding, M.A.; Chatterjee, A. *Handbook of Industrial Polyethylene and Technology: Definitive Guide to Manufacturing, Properties, Processing, Applications and Markets*; John Wiley & Sons: Hoboken, NJ, USA, 2017.
20. Mazur, K.; Jakubowska, P.; Romańska, P.; Kuciel, S. Green high density polyethylene (HDPE) reinforced with basalt fiber and agricultural fillers for technical applications. *Compos. Part B Eng.* **2020**, *202*, 108399. [[CrossRef](#)]
21. Anderson, K.S.; Hillmyer, M.A. The influence of block copolymer microstructure on the toughness of compatibilized polylactide/polyethylene blends. *Polymer* **2004**, *45*, 8809–8823. [[CrossRef](#)]
22. Thurber, C.M.; Xu, Y.; Myers, J.C.; Lodge, T.P.; Macosko, C.W. Accelerating Reactive Compatibilization of PE/PLA Blends by an Interfacially Localized Catalyst. *ACS Macro Lett.* **2014**, *4*, 30–33. [[CrossRef](#)]
23. Xu, Y.; Loi, J.; Delgado, P.; Topolkarayev, V.; McEneaney, R.J.; Macosko, C.W.; Hillmyer, M.A. Reactive Compatibilization of Polylactide/Polypropylene Blends. *Ind. Eng. Chem. Res.* **2015**, *54*, 6108–6114. [[CrossRef](#)]
24. Brito, G.F.; Agrawal, P.; Mélo, T.J.A.; Pinto, J.C.; Balaban, R. Mechanical and Morphological Properties of PLA/BioPE Blend Compatibilized with E-GMA and EMA-GMA Copolymers. *Macromol. Symp.* **2016**, *367*, 176–182. [[CrossRef](#)]
25. Quitadamo, A.; Massardier, V.; Santulli, C.; Valente, M. Optimization of Thermoplastic Blend Matrix HDPE/PLA with Different Types and Levels of Coupling Agents. *Materials* **2018**, *11*, 2527. [[CrossRef](#)] [[PubMed](#)]
26. Zolali, A.M.; Favis, B.D. Toughening of cocontinuous polylactide/polyethylene blends via an interfacially percolated intermediate phase. *Macromolecules* **2018**, *51*, 3572–3581. [[CrossRef](#)]
27. Ferri, J.M.; Garcia-Garcia, D.; Rayón, E.; Samper, M.D.; Balart, R. Compatibilization and Characterization of Polylactide and Biopolyethylene Binary Blends by Non-Reactive and Reactive Compatibilization Approaches. *Polymers* **2020**, *12*, 1344. [[CrossRef](#)] [[PubMed](#)]

28. Srithep, Y.; Nealey, P.; Turng, L.-S. Effects of annealing time and temperature on the crystallinity and heat resistance behavior of injection-molded poly(lactic acid). *Polym. Eng. Sci.* **2013**, *53*, 580–588. [[CrossRef](#)]
29. Wang, S.; Liu, B.; Qin, Y.; Guo, H. Effects of Processing Conditions and Plasticizing-Reinforcing Modification on the Crystallization and Physical Properties of PLA Films. *Membranes* **2021**, *11*, 640. [[CrossRef](#)]
30. Guo, H.; Rinaldi, R.G.; Tayakout, S.; Broudin, M.; Lame, O. The correlation between the mixed-mode oligo-cyclic loading induced mechanical and microstructure changes in HDPE. *Polymer* **2021**, *224*, 123706. [[CrossRef](#)]
31. Wellen, R.M.; Rabello, M.S.; Fachine, G.J.; Canedo, E.L. The melting behaviour of poly (3-hydroxybutyrate) by DSC. Reproducibility study. *Polym. Test.* **2013**, *32*, 215–220. [[CrossRef](#)]
32. Luna, C.B.B.; Ferreira, E.D.S.B.; Siqueira, D.D.; Filho, E.A.D.S.; Araújo, E.M. Additivition of the ethylene–vinyl acetate copolymer (EVA) with maleic anhydride (MA) and dicumyl peroxide (DCP): The impact of styrene monomer on cross-linking and functionalization. *Polym. Bull.* **2021**, *78*, 1–24. [[CrossRef](#)]
33. Barros, A.B.D.S.; Farias, R.D.F.; Siqueira, D.D.; Luna, C.B.B.; Araújo, E.M.; Rabello, M.S.; Wellen, R.M.R. The Effect of ZnO on the Failure of PET by Environmental Stress Cracking. *Materials* **2020**, *13*, 2844. [[CrossRef](#)]
34. Mohapatra, A.K.; Mohanty, S.; Nayak, S. Poly(lactic acid) and layered silicate nanocomposites prepared by melt mixing: Thermomechanical and morphological properties. *Polym. Compos.* **2012**, *33*, 2095–2104. [[CrossRef](#)]
35. da Silva, F.S.; Luna, C.B.B.; Siqueira, D.D.; Ferreira, E.D.S.B.; Araújo, E.M. From Waste to Reuse: Manufacture of Ecological Composites Based on Biopolyethylene/wood Powder with PE-g-MA and Macaíba Oil. *J. Polym. Environ.* **2021**, *29*, 1–17. [[CrossRef](#)]
36. Abdolrasouli, M.H.; Sadeghi, G.M.M.; Nazockdast, H.; Babaei, A. Polylactide/Polyethylene/Organoclay Blend Nanocomposites: Structure, Mechanical and Thermal Properties. *Polym. Technol. Eng.* **2014**, *53*, 1417–1424. [[CrossRef](#)]
37. da Silva, W.A.; Luna, C.B.B.; Melo, J.B.D.C.A.D.; Araújo, E.M.; Filho, E.A.D.S.; Duarte, R.N.C. Feasibility of Manufacturing Disposable Cups using PLA/PCL Composites Reinforced with Wood Powder. *J. Polym. Environ.* **2021**, *29*, 2932–2951. [[CrossRef](#)]
38. Ferreira, E.S.B.; Luna, C.B.B.; Siqueira, D.D.; Araújo, E.M.; De França, D.C.; Wellen, R.M.R. Annealing Effect on PLA/EVA Blends Performance. *J. Polym. Environ.* **2021**, *29*, 1–14.
39. Vrsaljko, D.; Macut, D.; Kovačević, V. Potential role of nanofillers as compatibilizers in immiscible PLA/LDPE Blends. *J. Appl. Polym. Sci.* **2015**, *132*, 132. [[CrossRef](#)]
40. Pai, F.-C.; Chu, H.-H.; Lai, S.-M. Reactive compatibilization of poly(lactic acid)/polyethylene octene copolymer blends with ethylene-glycidyl methacrylate copolymer. *J. Polym. Eng.* **2011**, *31*, 463–471. [[CrossRef](#)]
41. Gallego, R.; López-Quintana, S.; Basurto, F.; Núñez, K.; Villarreal, N.; Merino, J.C. Synthesis of new compatibilizers to poly (lactic acid) blends. *Polym. Eng. Sci.* **2014**, *54*, 522–530. [[CrossRef](#)]
42. Brito, G.F.; Agrawal, P.; Araújo, E.M.; De Melo, T.J.A. Polylactide/Biopolyethylene bioblends. *Polímeros* **2012**, *22*, 427–429. [[CrossRef](#)]
43. Huang, J.; Fan, J.; Yuan, D.; Zhang, S.; Chen, Y. Facile preparation of super-toughened polylactide-based thermoplastic vulcanizates without sacrificing the stiffness based on the selective distribution of silica. *Ind. Eng. Chem. Res.* **2020**, *59*, 9950–9958. [[CrossRef](#)]
44. Quiles-Carrillo, L.; Montanes, N.; Jorda-Vilaplana, A.; Balart, R.; Torres-Giner, S. A comparative study on the effect of different reactive compatibilizers on injection-molded pieces of bio-based high-density polyethylene/poly(lactide) blends. *J. Appl. Polym. Sci.* **2019**, *136*, 47396. [[CrossRef](#)]
45. Nascimento, W.A.; Silva, H.P.D.S.; Agrawal, P.; Lima, J.C.; de Melo, T.J.; Lira, H.D.L. Correlação entre propriedades mecânicas, reológicas e morfológicas de blendas PP/PA6 com adição de compatibilizantes. *Rev. Iberoam. Polim.* **2020**, *21*, 144–154.
46. Pruthikul, R.; Liewchirakorn, P. Preparation of Polypropylene Graft Maleic Anhydride (PP-g-MA) via Twin Screw Extrusion. *Adv. Mater. Res.* **2010**, *93–94*, 451–454. [[CrossRef](#)]
47. Mahesh, A.; Rudresh, B.; Reddappa, H. Potential of natural fibers in the modification of mechanical behavior of polypropylene hybrid composites. *Mater. Today Proc.* **2021**, *46*, 1–6. [[CrossRef](#)]
48. Luna, C.; Siqueira, D.; Ferreira, E.; Silva, W.; Nogueira, J.; Araújo, E. From Disposal to Technological Potential: Reuse of Polypropylene Waste from Industrial Containers as a Polystyrene Impact Modifier. *Sustainability* **2020**, *12*, 5272. [[CrossRef](#)]
49. Morais, D.D.D.S.; França, D.C.; Araújo, E.M.; Carvalho, L.H.D.; Wellen, R.M.R.; Oliveira, A.D.D.; Melo, T.J.A.D. Tailoring PS/PCL blends: Characteristics of processing and properties. *REM-Int. Eng. J.* **2019**, *72*, 87–95. [[CrossRef](#)]
50. Castro, L.; Oliveira, A.; Kersch, M.; Altstädt, V.; Pessan, L. Effects of mixing protocol on morphology and properties of PA6/ABS blends compatibilized with MMA-MA. *J. Appl. Polym. Sci.* **2016**, *133*, 1–8. [[CrossRef](#)]
51. Oliveira, A.D.D.; Larocca, N.M.; Pessan, L.A. Effect from the blending sequence on the properties of PA6/ABS blends compatibilized with SMA copolymer. *Polímeros* **2011**, *21*, 27–33. [[CrossRef](#)]
52. De Oliveira, A.D.; De Castro, L.D.C.; Beatrice, C.A.G.; Lucas, A.D.A.; Pessan, L.A. Effect of Maleic Anhydride Content in Properties of PA6/AES Blends Compatibilized with MMA-MA. *Mater. Res.* **2017**, *20*, 1630–1637. [[CrossRef](#)]
53. Luna, C.B.B.; Siqueira, D.D.; Ferreira, E.D.S.B.; Araújo, E.M.; Wellen, R.M.R. Reactive compatibilization of PCL/WP upon addition of PCL-MA. Smart option for recycling industry. *Mater. Res. Express* **2019**, *6*, 125317. [[CrossRef](#)]
54. Wang, L.; Wang, Y.-N.; Huang, Z.-G.; Weng, Y.-X. Heat resistance, crystallization behavior, and mechanical properties of polylactide/nucleating agent composites. *Mater. Des.* **2015**, *66*, 7–15. [[CrossRef](#)]

55. Yang, Y.; Zhang, L.; Xiong, Z.; Tang, Z.; Zhang, R.; Zhu, J. Research progress in the heat resistance, toughening and filling modification of PLA. *Sci. China Ser. B Chem.* **2016**, *59*, 1355–1368. [[CrossRef](#)]
56. Ferreira, E.D.S.B.; Luna, C.B.B.; Araújo, E.M.; Siqueira, D.D.; Wellen, R.M.R. Polypropylene/wood powder composites: Evaluation of PP viscosity in thermal, mechanical, thermomechanical, and morphological characters. *J. Thermoplast. Compos. Mater.* **2019**, *32*, 0892705719880958. [[CrossRef](#)]
57. Tao, Y.U.; Yan, L.I.; Jie, R.E.N. Preparation and properties of short natural fiber reinforced poly (lactic acid) composites. *Trans. Nonferrous Met. Soc. China* **2009**, *19*, 651–655.
58. Bezerra, E.B.; De França, D.C.; Morais, D.D.D.S.; Silva, I.D.D.S.; Siqueira, D.D.; Araújo, E.M.; Wellen, R.M.R. Compatibility and characterization of Bio-PE/PCL blends. *Polímeros* **2019**, *29*, 1–15. [[CrossRef](#)]
59. Siqueira, D.; Luna, C.; Ferreira, E.; Araújo, E.; Wellen, R. Tailored PCL/Macaiba fiber to reach sustainable biocomposites. *J. Mater. Res. Technol.* **2020**, *9*, 9691–9708. [[CrossRef](#)]
60. Siročić, A.P.; Hrnjak-Murčić, Z.; Jelenčić, J. The surface energy as an indicator of miscibility of SAN/EDPM polymer blends. *J. Adhes. Sci. Technol.* **2013**, *27*, 2615–2628. [[CrossRef](#)]
61. Tejada-Oliveros, R.; Balart, R.; Ivorra-Martinez, J.; Gomez-Caturla, J.; Montanes, N.; Quiles-Carrillo, L. Improvement of Impact Strength of Polylactide Blends with a Thermoplastic Elastomer Compatibilized with Biobased Maleinized Linseed Oil for Applications in Rigid Packaging. *Molecules* **2021**, *26*, 240. [[CrossRef](#)]
62. Moradi, S.; Yeganeh, J.K. Highly toughened poly(lactic acid) (PLA) prepared through melt blending with ethylene-co-vinyl acetate (EVA) copolymer and simultaneous addition of hydrophilic silica nanoparticles and block copolymer compatibilizer. *Polym. Test.* **2020**, *91*, 106735. [[CrossRef](#)]
63. Sangeetha, V.H.; Valapa, R.B.; Nayak, S.K.; Varghese, T.O. Investigation on the Influence of EVA Content on the Mechanical and Thermal Characteristics of Poly(lactic acid) Blends. *J. Polym. Environ.* **2016**, *26*, 1–14. [[CrossRef](#)]